Acta Biochim Biophys Sin 2013, 45: 845–856 | © The Author 2013. Published by ABBS Editorial Office in association with Oxford University Press on behalf of the Institute of Biochemistry and Cell Biology, Shanghai Institutes for Biological Sciences, Chinese Academy of Sciences. DOI: 10.1093/abbs/gmt089.
Advance Access Publication 26 August 2013

Original Article

Physicochemical study of a novel chimeric chitinase with enhanced binding ability

Soheila Matroodi, Mohammadreza Zamani, Kamahldin Haghbeen*, Mostafa Motallebi*, and Saeed Aminzadeh

National Institute of Genetic Engineering and Biotechnology, PO Box: 149651/161, Tehran, Iran
*Correspondence address. Tel: +98-21-44580372; Fax: +98-21-4580399; E-mail: Kamahl@nigeb.ac.ir (K.H.); Motalebi@nigeb.ac.ir (M.M.)

Chitinases are slow-reacting but important enzymes as they are anticipated to have diverse applications. The role of a chitin-binding domain (ChBD) in enhancing the quality of binding is essential information for purposeful engineering of chitinases. The idea of making hybrid chitinases by fusing a known ChBD to a chitinase, which naturally lacks ChBD is of interest especially for bio-controlling purposes. Therefore, in the present study, the ChBD of *Serratia marcescens* chitinase B was selected and fused to the fungal chitinase, *Trichoderma atroviride* Chit42. Both Chit42 and chemric Chit42 (ChC) showed similar activity towards colloidal chitin with specificity constants of 0.83 and 1.07 min^{-1}, respectively, same optimum temperatures (40°C), and similar optimum pH (4 and 4.5, respectively). In the presence of insoluble chitin, ChC showed higher activity (70%) and obtained a remarkably higher binding constant (700 times). Spectroscopic studies indicated that chimerization of Chit42 caused some structural changes, which resulted in a reduction of α-helix in ChC structure. Chemical and thermal stability studies suggested that ChC had a more stable structure than Chit42. Hill analysis of the binding data revealed mixed-cooperativity with positive cooperativity governing at ChC concentrations below 0.5 and above 2 μM in the presence of insoluble chitin. It is suggested that the addition of the ChBD to Chit42 affords structural changes which enhance the binding ability of ChC to insoluble chitin, improving its catalytic efficiency and increasing its thermal and chemical stability.

Keywords chitin-binding domain; chimeric chitinase; kinetic; binding; structure

Received: February 9, 2013 Accepted: May 9, 2013

Introduction

Chitin, the second most abundant biopolymer in nature, is a linear homopolymer of *N*-acetylglucosamine (GlcNAc) which is a principal structural component in the cell walls of fungi, insect exoskeleton, and the shells of crustaceans [1]. It is degraded by chitinases which are widely distributed in viruses, bacteria, fungi, plants, and animals. A great deal of interest in chitinases has been generated because of their applications in the biocontrol of plant pathogenic fungi [2,3], production of chito-oligosaccharides [4], and mycolytic enzyme preparation [5].

To increase tolerance to diseases caused by biotrophic and necrotrophic fungal pathogens, the overexpression of chitinases from a wide range of donor organisms has been examined in a variety of plant species. However, chitinase-derived resistance is rarely high enough to be pursued in commercial sectors [3,6]. In addition, chitinases originating from mycoparasitic biocontrol agents have proven to be more effective for enhancing fungal disease resistance in transgenic plants; most notably *Trichoderma sp.* with their ability to exhibit higher anti-fungal activity than plant chitinases have proven to be more effective for enhancing fungal disease resistance in transgenic plants [7,8].

Fungal chitinases are members of glycosyl hydrolases, which mostly belong to the GH18 family [4]. A few of them contain a chitin-binding domain (ChBD), which facilitates efficient degradation of insoluble chitin [9–12]. Increasing interest in this feature and other physiochemical properties of chitinases has been stimulated by the possible involvement of these enzymes in the biocontrol of chitinous pests and invaders [13].

Chit42 is an endochitinase from *Trichoderma atroviride* PTCC 5220 that is expected to play a key role in biocontrol activities against plant pathogens [12]. This enzyme carries no ChBD naturally, but some hybrid chitinases with stronger chitin-binding capacity have been produced by fusing either a ChBD, from *Nicotiana tabacum*, or a cellulose-binding domain (CeBD), from the cellobiohydrolase II gene of *T. reesei*, to a similar Chit42 chitinase from *T. harzianum*. The chimeric chitinases produced in recombinant bacteria have higher hydrolytic activity than the native chitinases on chitin-rich fungal cell walls. However, the hybrid chitinases are very unstable and tend to lose the substrate-binding domain [14]. Similarly, Limon *et al.* [15] has demonstrated the positive impact of adding a CeBD on increasing the

hydrolytic activity of *T. harzianum* Chit42 towards insoluble substrate such as chitin-rich fungal cell walls.

The current literature on this subject fails to provide a definitive explanation of the effect of different ChBD(s) on the physicochemical properties of chitinases such as Chit42. In the present study, to shed a light on this subject, a different ChBD from a *Serratia marcescens* chitinase B was selected and fused to the fungal chitinase, *T. atroviride* Chit42. The catalytic domain of *S. marcescens* chitinase B showed high structural similarity to that of Chit42 *T. atroviride*. Investigations were carried out to analyze the physicochemical activities of the new chimeric chitinase (ChC).

Materials and Methods

Bacterial strains, plasmids, and media

Escherichia coli BL21 (DE3) and DH5α (Invitrogen, Grand Island, USA) were used. *Serratia marcescens* (PTCC 1607) was obtained from Persian Type Collection Culture (Tehran, Iran). Bacteria were grown in Luria Bertani medium at 37°C. pUC19 vector (Novagen, Darmstadt, Germany) was used for routine cloning and pET-26b(+) (Novagen) was used as an expression vector. All chemicals and antibiotics were purchased from Merck (Darmstadt, Germany), unless otherwise stated. DNA modifying enzymes were obtained from Roche Biochemical and Fermentase (Waltham, USA).

Design and construction of hybrid chitinase

Molecular biology methods such as polymerase chain reaction (PCR), agarose gel electrophoresis, competent cells preparation, plasmid isolation, restriction digestion, ligation, and transformation were performed as outlined by Sambrook *et al.* [16]. To add 6× His-tag encoding region to the 3′-end of cDNA for the purification of Chit42, the 1278 bp cDNA *Chit42* (accession number DQ132792.1) was PCR-amplified by using primers chS5 (5′-ggaagacaaca tgtctcctgtaactgcaaacg-3′) and CDP42 (5′-cgctcgaggttgagacc gcttcgg-3′) with *Pfu* DNA polymerase. The amplicon with deletion of stop codon was cloned into the *Nco*I and *Xho*I sites of pET 26b(+) to yield pETSM1.

To create a chimeric gene containing linker-ChBD-6× His-tag at the C-terminal end of Chit42 cDNA, the fragment containing *Chit42* cDNA (F1 fragment) was amplified using primers chS5 and R42 (5′-gtcgtcgtagtcgttgagaccgcttcgg atgtt-3′). This fragment contained the coding sequence of the mature protein of Chit42 (1278 bp) without its signal peptide. The second fragment containing linker and ChBD (F2 fragment) of chitinase B (accession number X15208) was amplified using the genomic DNA of *S. marcescens* as template and Fchbd2 (5′cgaagcggtctcaacgactacgacgacag ccagc3′) and Rchbd2 (5′cgctcgagcgccaggcggcccac3′) as primers. This fragment contained 33 bp as linker and 189 bp as ChBD [17].

Each PCR mixture (50 μl) contained a DNA template (14 μg), dNTP (25 mM), primer (400 nM), *Pfu* DNA polymerase (1.25 U), and $MgSO_4$ (1.5 mM). For each set of primers, the PCR program consisted of 30 repetitive cycles with a strand separation step at 94°C for 1 min, an annealing step at 58°C for 1 min, and an elongation step at 72°C for 1 min. Fragments F1 and F2 were purified by using a PCR product purification kit (Roche, Homburg, Germany) and fused together in the second PCR step. R42 and Fchbd2 primers contained a 12-nt long 5′-extension complementary to the end of the adjacent fragment of the hybrid gene that was necessary to fuse different fragments together.

For overlap extension PCR (SOEing PCR), equimolar amounts of each fragment were mixed in the absence of additional primers by using dNTP (50 mM), *Pfu* DNA polymerase (2.5 U), and $MgSO_4$ (1.5 mM) according to a previous report [18].

The PCR program consisted of seven repetitive cycles was carried out with a denaturation step (94°C, 1 min), an annealing step (52°C, 1 min), and an elongation step (72°C, 1.5 min). The fusion product was subsequently amplified by using primers chS5 and Rchbd2 in 50 μl of PCR mixture containing DNA template (14 μg), dNTP (25 mM), primer (400 nM), *Pfu* DNA polymerase (1.25 U), and $MgSO_4$ (1.5 mM). A similar PCR program was employed here again with the exception that the annealing temperature was set to 60°C. The chimeric gene was purified and cloned into pET26b(+) with *Nco*I and *Xho*I sites to yield pETCSM2. The nucleotide sequence of the chimeric gene was verified by DNA sequencing. The chimeric construct was then transferred to *E. coli* BL21(DE3).

Expression and purification of Chit42 and hybrid protein

The expression of both *chit42* and the hybrid gene that had been subcloned into pET26b(+) was under the control of T7 promoter. The optimal condition of IPTG, 1 mM, and incubation at 28°C for 16 h were employed for the protein expression. The expression resulted in corresponding proteins carrying 6× His-tag at the C-terminal. 6× His-tag was added to the C-terminal of both proteins to facilitate their purification [19]. Accordingly, the recombinant proteins were purified by using Nickel–nitrilotriacetic acid (Ni–NTA) resin under native conditions. Briefly, cell pellet (50 ml) was resuspended in 5 ml of lysis buffer containing 50 mM NaH_2PO_4, pH 8.0, 300 mM NaCl, and 10 mM imidazole. The suspension was then sonicated 15 times at 30 s on/45 s off, 70 W. The resultant was centrifuged at 8000 rpm for 20 min. The supernatant was separated and loaded on a 1-cm high Ni–NTA affinity column. The column was washed with lysis buffer containing 40 mM imidazole and the bound protein was eluted with a similar buffer containing 250 mM imidazole. The purification procedure was carried out at 4°C and the purified hybrid

protein, R42, was subjected to 12% sodium dodecyl sulfate–polyacrylamide gel electrophoresis (SDS–PAGE). The pI of Chit42 or ChC was determined by the isoelectric focusing method introduced in our previous work [20].

Western blot analysis

Purified protein from SDS–PAGE was transferred to a polyvinylidene difluoride (PVDF) membrane (Roche) by using transfer buffer containing 39 mM glycine, 48 mM Tris-base, 0.037% SDS, and 20% methanol with Bio-Rad Mini Protean II System (Bio-Rad, Hercules, USA). The PVDF membrane was incubated in blocking buffer containing 3% skim milk powder for 2 h and then incubated with mice anti-His-tag IgG (1 : 1000) in PBS-T (PBS containing 0.05% Tween 20) with gentle shaking for 3 h at 37°C. The membrane was washed with PBS-T three times and detection was carried out by using 4-chloronaphthol. Chromogenic reaction was stopped by rinsing the membrane twice with distilled water.

Enzyme assay

Chitinase assay was carried out as described by Bruce *et al.* [21] with some modifications. Briefly, four tubes were set up for each purified enzyme. Each tube contained purified enzyme (80 μg in 200 μl volume) and substrate (200 μl). Crab-shell chitin (practical grade; Sigma-Aldrich, St Louis, USA) and its colloidal were used as substrate. The substrate solution was made by dissolving 3.8 mg of colloidal chitin in 1 ml of McIlvaine citrate phosphate buffer at pH 5. The tube A of each set was boiled for 10 min to destroy enzyme activity before incubating all tubes at 37°C for 1 h. After incubation, all tubes were boiled for 10 min. To assay, 0.1 ml of 0.8 M potassium tetraborate was added to 0.4 ml of each sample (tubes A–D). The resulting mixtures were boiled for 3 min then cooled to room temperature and mixed with 3 ml of *p*-dimethylaminobenzaldehyde reagent (DMAB). The mixtures were maintained at room temperature for 20 min before subjecting to the absorbance reading at 544 nm. The reagent was made by dissolving 10 g DMAB in a mixture containing 12.5 ml of 10 N HC1 and 87.5 ml of glacial acetic acid. The reagent was stored at 2°C and diluted 1 : 10 with glacial acetic acid before use. Tube A was used as blank. Calibration curve obtained by reading the absorbance at 544 nm of final reaction products of commercial GlcNAc with DMAB under the above conditions. The amount of commercial GlcNAc was 0, 1.6, 1.9, 3.1, 3.9, 6.25, 7.8, 12.5, 15.6, 25, 31.25, 40, 50, 62.5, 70, 80, and 90 μg per 0.5 ml of McIlvaine buffer, pH 5, respectively. All the spectrophotometric measurements were carried out by using an Analytik Jena spectrophotometer (Bioline SPECORD 210; Jena, Germany). Production of 1 μmol of colorful product per hour was considered as one unit of activity. Colloidal chitin was obtained from an acidic treatment of crab-shell chitin according to the previously described procedure [22].

Velocity curves and inhibition studies

Using the method mentioned above, velocity curves for Chit42 and ChC were obtained by measuring the enzymatic reaction rate of a constant concentration of each enzyme (87 μg per 0.5 ml of reaction mixture) in the presence of various amounts of colloidal chitin (0.1, 0.5, 1, 1.5, 2, and 3 mg/ml) at 37°C in citrate buffer (0.2 M, pH 5). Similarly, the inhibition studies were carried out in the presence of a constant amount of each enzyme and various amount of colloidal chitin (0.5, 1.5, and 3 mg/ml) with caffeine as inhibitor (0, 1, 2, 3.5, and 5 mM). All kinetics data reported in this work were based on the averages of at least three tests.

Ph and temperature optima and thermal stability

The pH optimum of the purified enzymes was determined after incubating each enzyme with colloidal chitin in various pH buffers containing sodium citrate (pH 3.0–5.0), sodium acetate (pH 5.0–6.0), sodium phosphate (pH 6.0–8.0), glycine–NaOH (pH 8.0–10.0), and sodium phosphate (pH 10.0–11.0).

Temperature optimum was determined by performing standard assay in the presence of colloidal chitin at temperatures ranging from 20 to 80°C. The thermal stability was also determined by incubating the enzymes for 1 h at temperatures ranging from 20 to 80°C in sodium acetate buffer (50 mM, pH 5) and then measuring the remaining activity at 37°C.

Binding assays

To evaluate the binding activity, 1 mg of dried and ground crab-shell chitin was incubated with different concentrations of each enzyme (0.25–4 μM) in 1 ml of 30 mM phosphate buffer, pH 6.0, on a gel shaker of 450 rpm for 1 h at 4°C. After incubation, the mixtures were centrifuged at 13 000 rpm for 10 min at 4°C. To obtain the concentration of non-bound protein, extinction coefficient at 280 nm for Chit42 and ChC was 95 400 and 90 400 $M^{-1} \cdot cm^{-1}$, respectively. Therefore, the amount of non-bound protein was determined by reading the absorbance of each solution at 280 nm. The protein content of each solution was double-checked by the Bradford method.

Protein denaturation studies

Denaturation curves of Chit42 and ChC in the presence of dodecyl trimethylammonium bromide (DTAB) were obtained by measuring the absorbance changes at 280 nm of each protein solution containing 0.3 mg/ml enzyme in a 1-cm cuvette thermostated at 20 ± 0.1°C. All measurements were carried out after enzyme solution and DTAB had been incubated for over 5 min and the absorbance was not changing. The standard Gibbs free energy of denaturation (ΔG°), as a criterion of conformational stability of a protein, was

determined according to the theory thoroughly described in our previous work [23].

Circular dichroism

Experiments were performed with a Jasco J-700 spectrophotometer (JASCO, Easton, USA). The results were expressed as ellipticity (θ) ($\mathrm{deg \cdot cm^2 \cdot dmol^{-1}}$). The spectrophotometer was equipped with a temperature programmer for controlling the rate of temperature change. The scan rate was 2 K/min in melting experiments. The data were smoothed by applying the Jasco J-700 software including a fast Fourier-transform noise reduction routine, which allowed for enhancement of most of the noisy spectra without distorting the shapes of their peaks. Far-UV studies were performed for both enzymes of 0.1 mg/ml, while near-UV experiments were performed with 2 mg/ml of two enzymes. All the fluorescence measurements were carried out on a Cary Eclipse fluorescence spectrophotometer (Varian, Manasquan, USA) at room temperature.

Results

Construction of Chit42 and chimeric chitinase

To prepare ChC, Chit42 of *T. atroviride* was first made according to the previously reported procedure [12]. ChBD was made by using specific primers and amplified from the genomic DNA of *S. marcescens*. SOEing PCR analysis showed that ChBD was inserted to the C-terminal of Chit42 [**Fig. 1, Fig. 2(A)**].

The molecular weight of Chit42 and ChBD was about 42 and 12 kD, respectively, a band close to 54 kD was expected to be seen on SDS–PAGE gel [**Fig. 2(B)**]. Western blot assay confirmed the right expression of both proteins [**Fig. 2(C)**]. The pI value was determined to be 3.66 and 3.95 for ChC and Chit42, respectively, by isoelectric focusing assay. The lower pI value of ChC could be ascribed to the existence of four more aspartic acid residues in the new construct (**Fig. 1**).

Kinetics of chitinase activity

Figure 4 showed the calibration curve which was obtained from the reaction of various concentrations of commercial GlcNAc with Ehrlich's reagent. The extinction coefficient of final colorful product was 12 100 $\mathrm{M^{-1}\,cm^{-1}}$ at 544 nm (**Fig. 4**). The velocity curves of both Chit42 and ChC were showed in **Fig. 5**. The kinetic parameters was summarized in **Table 2** extracted from double-reciprocal analysis of the kinetic data.

Inhibition studies were carried out by using caffeine as the inhibitor. An IC_{50} value was determined to be ~4 mM for both Chit42 and ChC [**Fig. 6(A)**] at a constant concentration of substrate. Kinetic studies on the inhibition of Chit42 and ChC at various concentrations of colloidal chitin were illustrated in **Fig. 6(B,C)**.

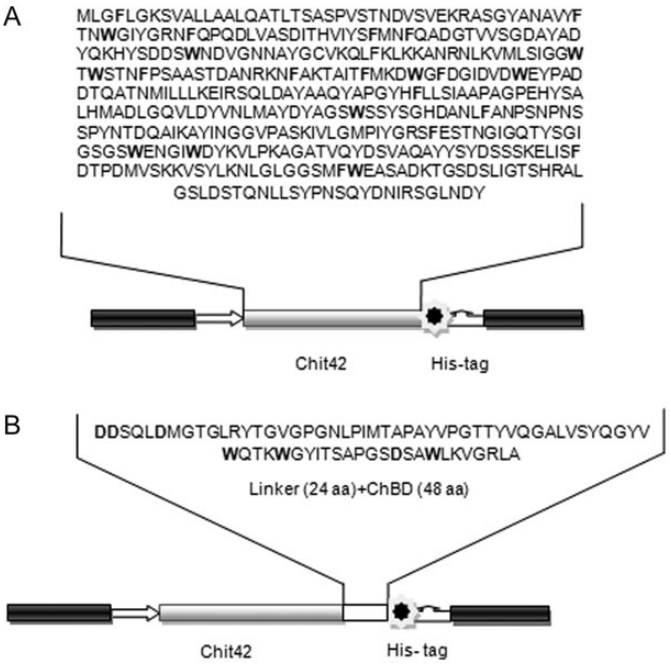

Figure 1 Scheme of gene construction for ChC (A) That part of pETSM1 which contains Chit42 amino acid sequences and 6× His-tag. Capital letters shows the aromatic amino acids. (B) That part of pETCSM2 which contains ChBD and 6× His-tag. Capital letters shows aspartic acid and tryptophan residues.

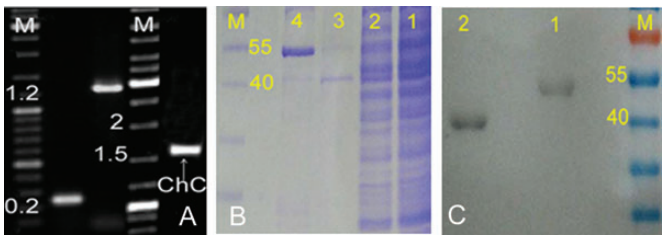

Figure 2 Identification of expressed proteins (A) PCR products including fragment F2 (225 bp), fragment F1 (1278 bp), and ChC obtained from overlap extension PCR (1497 bp). M, mixed ladder (kb). (B) SDS–PAGE of the expressed proteins and purified hybrid chitinase with 6× His-tag. 1, products before column chromatography; 2, flow-through; 3, washed proteins; 4, purified ChC after elution; M, protein marker (kDa). (C) Western blot analysis of Chit42 and ChC using anti 6× His-tag antibodies. 1, ChC; 2, Chit42; M, protein marker (kDa).

Structural studies

In the present work, SWISS-MODEL server was used for protein structure prediction based on homology modeling. Results showed that Chit42 and ChC shared sequence similarity with template by 73% and 65%, respectively (data not shown). **Figure 7** showed the predicted structures for these enzymes obtained from protein structure homology modeling. To evaluate the predicted structure, the solutions with

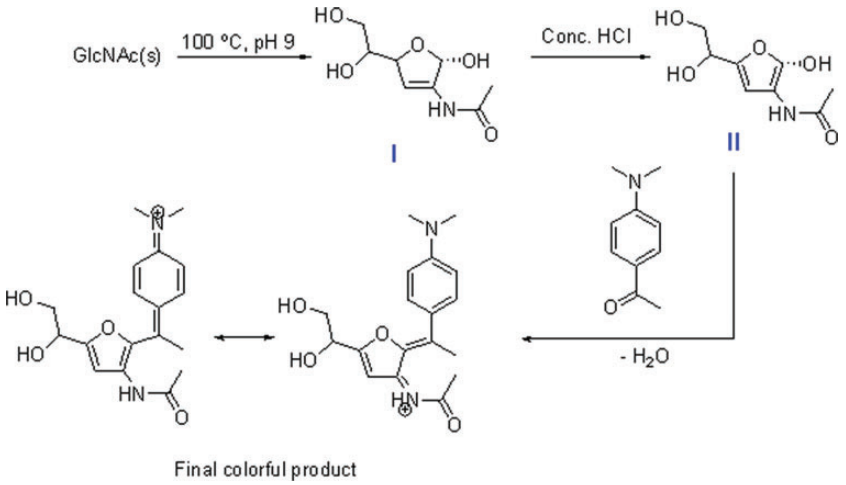

Figure 3 Calibration curve for measuring the final products of the reactions of known amounts of commercial GluNAc with Ehrlich's reagent under different circumstances.

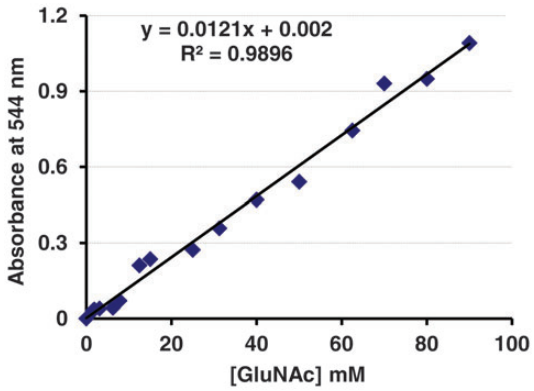

Figure 4 Proposed mechanism and chemical structure of the final product of the assaying method [25] employed in this study.

equal concentrations of Chit42 and ChC were subjected to fluorescence, near-UV, and far-UV circular dichroism (CD) spectroscopic examinations. Results of these studies are shown in **Fig. 8**.

Binding studies

Chitinase activity proceeded very slowly at temperature below 4°C. Considering a steady state for chitinase reaction, it has been assumed that the majority of chitinase molecules is at a state of binding equilibrium at this temperature [15]. Using this condition, the binding of Chit42 and ChC to insoluble chitin was studied. Data were illustrated in **Fig. 9**.

Ph, temperature profiles, and stability

Figure 10(A,B) showed the optimal pH and temperature for both Chit42 and ChC with colloidal chitin as a substrate. Thermal and chemical stability assays showed that ChC had a higher structural and functional stability [**Fig. 10(C,D)**] and this chimeric enzyme maintained ~30% of its original activity at temperature >50°C and could tolerate a higher concentration of DTAB, 2 mM, before denaturing.

Discussion

To establish a better understanding of the mechanism by which ChBD influences the bio-physicochemical features of a chimeric chitinase, ChBD of a soil bacterium, *S. marcescens*, was selected to be associated with Chit42 which was obtained from the biocontrol fungi, *T. atroviride*. **Fig. 2(B,C)** showed successful preparation of both Chit42 and the chimeric chitinase.

In order to investigate the influence of the addition of ChBD to a chitinase on its binding, it was necessary to compare the enzymatic activities of Chit42 and ChC in the presence of the natural substrate. Therefore, natural crab-shell chitin and its colloidal form were used as substrate. Since the average molecular weight of these substrate is not known, it would be useless to compare the Apparent K_m (K_mApp) values obtained in this work with those of soluble substrate such as $(GlcNAc)_4$ [24] which has known molecular weight. Moreover, the results of kinetic and binding studies will help to understand how physicochemical features of Chit42 change after the addition of ChBD.

Chitinase activity was first assayed using a spectrophotometric method by Morgan and Elson in 1933 and has been developed by others in later work [25,26]. The method was designed to measure the formation of a chromophoric substance with λ_{max}(s) at 544 and 585 nm, which is produced from the reaction of the cyclic intermediate of GlcNAc with Ehrlich's reagent, DMAB, as showed in **Fig. 3**, in acidic pH [26]. The method has some important advantages. It is based on measuring the products of enzymatic hydrolysis of chitins. Insoluble and colloidal chitin can be easily separated from reaction medium. The released GlcNAcs, dimer or

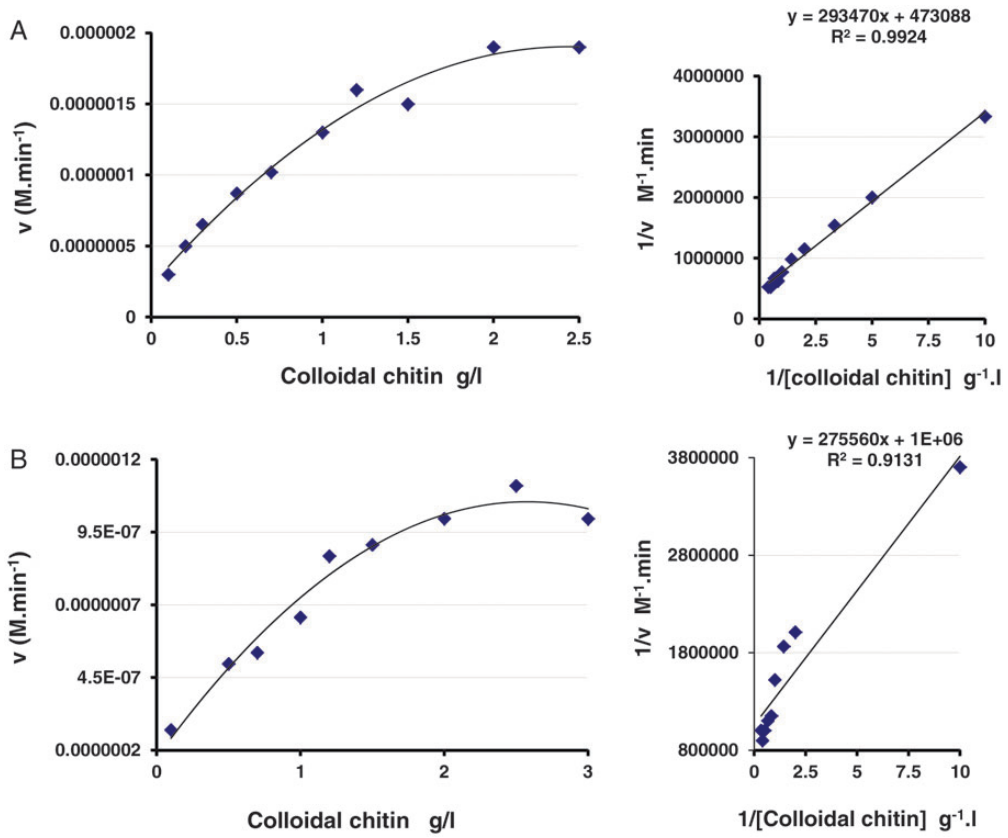

Figure 5 Velocity curves of Chit42 (A) and ChC (B) obtained in the presence of colloidal chitin Inset graphs are Lineweaver–Burk plots of the corresponding kinetic data [*S*] shows the concentration of the employed chitinase.

Table 1 Enzyme activity and specific activity of Chit42 and ChC in the presence of insoluble chitin

	Chit42	Chimeric chitinase
Activity (U/ml)	1.4 ± 0.3	2.4 ± 0.1
Specific activity (U/mg)	4 ± 0.7	6.87 ± 0.2

Means within column are significantly different ($P > 0.05$). All the enzymatic reactions were carried out in the presence of a constant amount of enzyme (86 μg) and insoluble chitin (1 mg/ml) in citrate buffer (0.2 M, pH 5) at 37°C. A unit of enzyme is equal to production of 1 μM/min of the colorful product illustrated in **Fig. 3**.

Table 2 Enzyme activity and specific activity of Chit42 and ChC in the presence of a constant amount of colloidal chitin (3.8 mg · ml^{-1})

	Chit42	Chimeric chitinase
Activity (U/ml)	7.76 ± 0.6	10.0 ± 0.7
Specific activity (U/mg)	22.7 ± 1.6	28.57 ± 2.2
Double reciprocal method		
K_mApp (M)	0.62	0.27
V_{max} (μmol l^{-1} · min^{-1})	2.11	1
Specificity constant (min^{-1})	0.83	1.07

Means within column are significantly different ($P > 0.05$). Kinetic parameters are extracted from the analyses of the velocity curves illustrated in **Fig. 5** using two different methods. All enzymatic reactions were carried out in the presence of a constant amount of enzyme (86 μg) in citrate buffer (0.2 M, pH 5) at 37°C.

larger, are hydrolyzed further under boiling conditions in alkaline medium and are turned into a heterocyclic compound (**Fig. 3**, structure I). The final product of GlcNAc with DMAB has a characteristic UV–visible spectrum, which can be employed for assaying purposes [26].

Comparing the results in **Tables 1 and 2**, the chitinase reaction was expectedly slower when insoluble chitin was used as substrate. These results were similar to the data reported by Shubakov and Kucheryavykh [27], who have observed chitinolytic activity ranging from 0.2 to 4.2 U/mg for different filamentous fungi in the presence of colloidal chitin. Kim and Ji reported a specificity constant of 0.91 for *Streptomyces griseus* chitinase in the presence of insoluble chitin [28]. However, from the activity point of view, both Chit42 and ChC seemed to be more efficient than *S. griseus* chitinase.

Data from **Table 1** revealed that ChC was more active than Chit42 by ~70% towards insoluble chitin. This difference decreased to only 28% in the presence of colloidal substrate (**Table 2**), which suggested that the association of

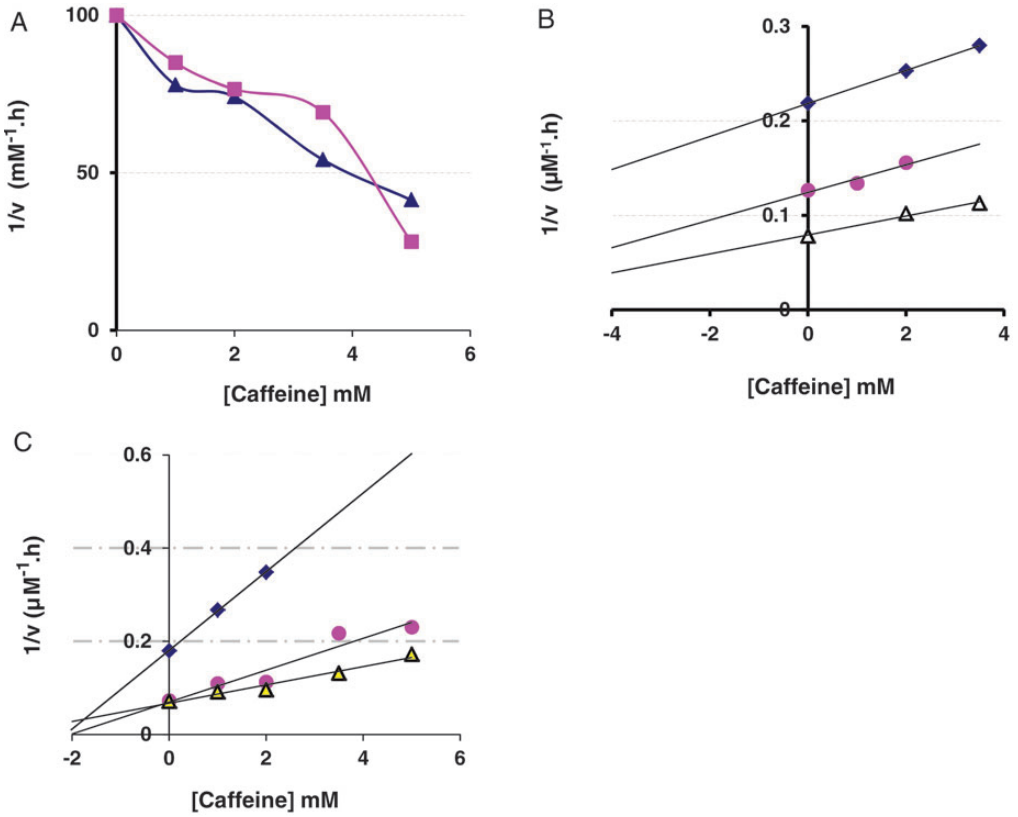

Figure 6 Enzymatic activity of Chit42 and ChiC (A) Relative activity of Chit42 (filled square), and ChC (filled triangle) in the presence of 3 mg/ml of colloidal chitin and various amounts of caffeine. Dixon plots of the kinetic results of inhibition of Chit42 (B) and ChC (C) in the presence of 0.5 (filled rhombus), 1.5 (filled circle), and 3 (filled triangle) mg/ml of colloidal chitin and various amounts of caffeine. All the enzymatic reactions were carried out in citrate buffer (0.2 M, pH 5) at 37°C.

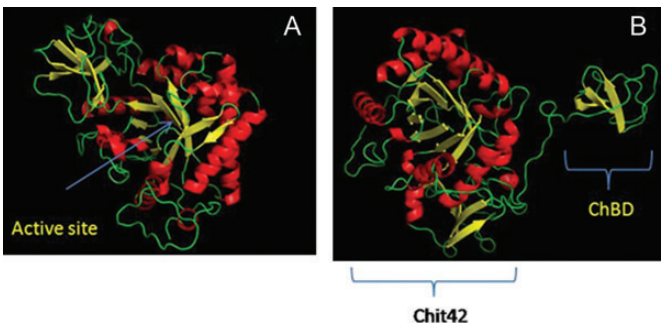

Figure 7 Predicted structures for Chit42 (A) and ChC (B) by SWISS-MODEL server using the homology modeling method.

ChBD to Chit42 increased the selectivity of the enzyme towards the insoluble substrate. Limon *et al.* [15] added a ChBD, which was obtained from *N. tabacum*, to Chit42 and observed an activity increase of ~36% in presence of insoluble chitin. But Fan *et al.* [13] constructed a chimeric chitinase from the silkworm ChBD and *Beauveria bassiana* chitinase, which showed a 5.5-fold increase in enzymatic activity in the presence of powdered chitin. Data in **Table 2** also suggested a 2-fold increase in the affinity of ChC with colloidal substrate even though Chit42 and ChC both showed similar specificity constants with colloidal chitin. It has been understood that the addition of a ChBD to a chitinase does not remarkably improve its enzymatic activity towards soluble chitin. Data reported by Limon *et al.* [15] indicated a decrease in hybrid chitinase activity in the presence of soluble chitin. Fan *et al.* [13] reported, at most, a 2-fold specificity constant for the chimeric enzyme in the presence of soluble chitin.

The deviation from linearity observed in the double-reciprocal analysis of ChC kinetic data [**Fig. 5(B)**] was important to be noted. Since the double-reciprocal method of Lineweaver–Burk has been criticized for an imbalanced weighing of data collected at lower concentrations of substrate [29], the kinetic data were also analyzed by Eadie–Hofstee method. Although the obtained K_mApp values of Chit42 and ChC were similar (0.66 and 0.33 M) to those resulted from Lineweaver–Burk method, marked differences in linearity were unveiled. Eadie–Hofstee analysis showed 65% linearity for ChC kinetic data, while 96% for Chit42 (data not shown). Deviations from linearity in Eadie–Hofstee analysis were considered as a strong indication of non-Michaelis–Menten behavior of an enzyme [30]. Considering these results, it was

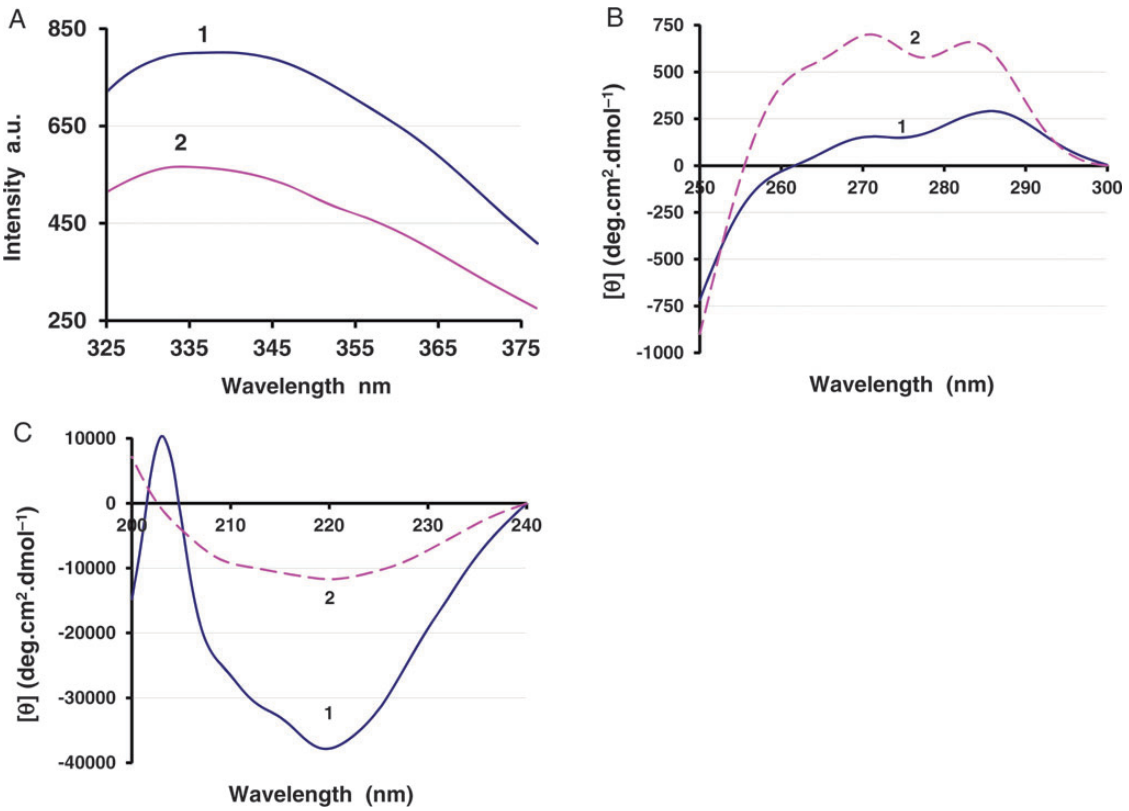

Figure 8 Structural analysis for Chit42 and ChC (A) Intrinsic fluorescence emission spectra of 0.5 μM Chit42 (**1**) and ChC (**2**) using an excitation wavelength of 280 nm. (B) Near-UV CD spectra as ellipticity (θ) of 2 mg/ml of Chit42 (**1**) and ChC (**2**). (C) Far-UV CD as ellipticity (θ) of 0.1 mg/ml of Chit42 (**1**) and ChC (**2**). All the spectra were recorded from enzyme solutions in modified elution buffer [NaH_2PO_4 (50 mM), pH 8.0, NaCl (300 mM)] at 20°C.

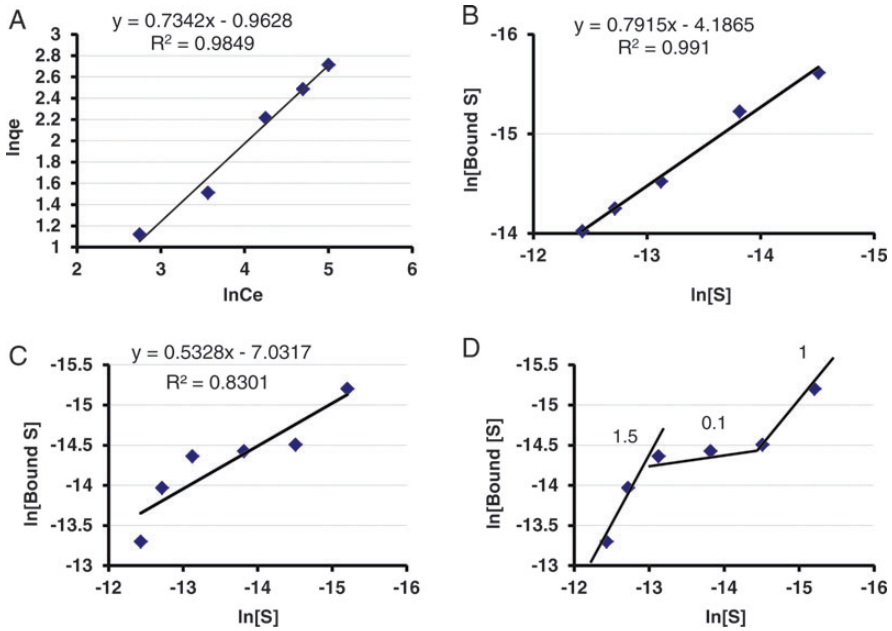

Figure 9 Binding activity of Chit42 and ChC (A) Analysis of the binding data of Chit42 in the presence of insoluble chitin using Freundlich equation. Hill plots of the binding data of Chit42 (B) and ChC (C) in the presence of insoluble chitin. (D) Slope analysis of various parts of ChC Hill plot illustrated in (C). [*S*] is the concentration of the employed chitinase in the binding experiments.

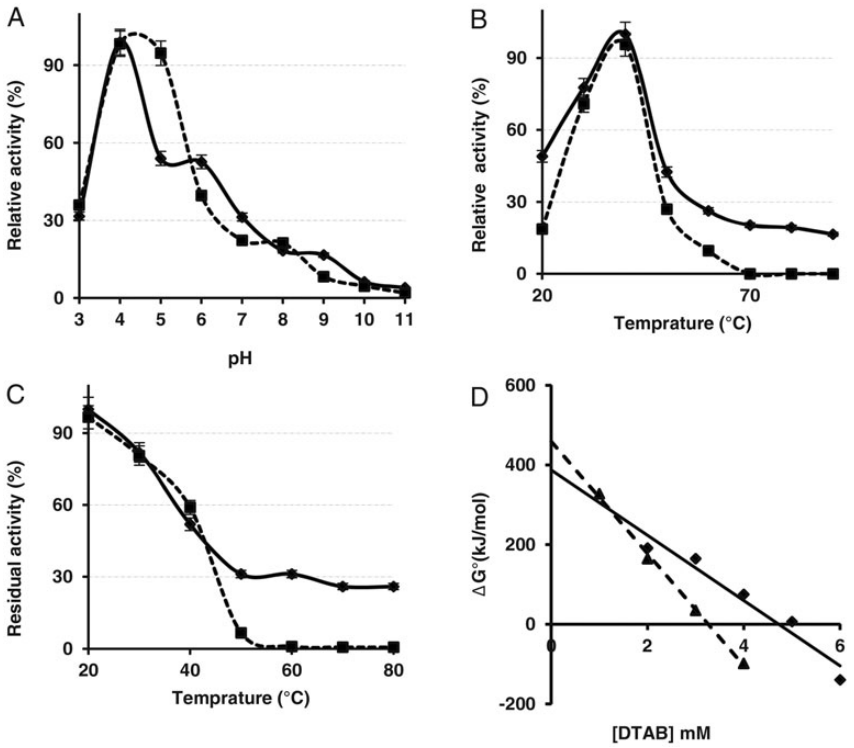

Figure 10 Enzyme kinetics of Chit42 and ChC Profiles of chitinase activity versus pH (A) and temperature (B). (C) Residual activity of the enzymes after maintaining each enzyme at various temperatures for 1 h. (D) Linear extrapolation method for calculation of free energy in the presence of DTAB [21]. Colloidal chitin was used as a substrate in all of these experiments. Chitinase activities of Chit42 (filled square) and ChC (filled triangle) were measured in citrate buffer (0.2 M, pH 5).

understood that the addition of ChBD to Chit42 obviously increased the complexity of its kinetics. It is noteworthy to mention that Bade and Stinson [31] had obtained a sigmoidal velocity curve for the tobacco hornworm chitinase. To find a better view about the kinetics natures of Chit42 and its chimera, the inhibition of both enzymes was studied using colloidal chitin as substrate with caffeine as inhibitor. It has been shown that methylxanthine derivatives, such as caffeine, are able to inhibit chitinase [32].

Result of the kinetics of inhibition indicated similar affinity of both enzymes for caffeine. Although Rao *et al.* [33] used a soluble substrate, 4-methylumbelliferyl-β-D-*N*,*N*′-diacetylchitobiose, in their study on the inhibition of a bacterial chitinase, they obtained an IC_{50} value of 0.5 mM for caffeine. Considering the result of the present work, it could be concluded that caffeine is a moderate inhibitor for chitinases.

The Dixon analyses did not follow linearity over the examined range of inhibitor concentration. Consequently, to obtain linear trends, it was necessary to drop out some of the data illustrated in **Fig. 6(B,C)**. In contrast to the results reported by Rao *et al.*, the mode of inhibition for both Chit42 and ChC was dependent on the concentration of both caffeine and substrate. Although these Dixon plots were not suitable for extracting the inhibition parameters, they clearly disclosed the complex nature of Chit42 and ChC kinetics. For instance, studying the inhibition of Chit42 at concentrations of caffeine up to 4 mM resulted in a Dixon plot showing a kind of uncompetitive mode of inhibition [**Fig. 6(B)**]. But increasing the inhibitor concentration beyond 5 mM tended to change the mode to mixed inhibition (data not shown). In a similar way, as illustrated in **Fig. 6(C)**, inhibition at higher concentrations of substrate produced results which exhibited a competitive mode in a Dixon plot where results obtained at lower concentrations of substrate tended to form a mixed-inhibition graph. These observations disclosed the non-Michaelis–Menten nature of the chitinase activities of both Chit42 and the hybrid chitinase which is normally interpreted in terms of allostery and cooperativity [30]. However, in the case of chitinase, the assumption of one enzyme and one substrate may be invalid [34]. Both Chit42 and ChC are monomer proteins but react with a substrate that can be considered as a macromolecule by itself. The observed complexity in the kinetics of these enzymes might in part be due to the complexity of the binding processes prior to the enzymatic reaction.

Before analyzing the results of binding studies, it is instructive to survey for structural changes of Chit42 after ChBD addition. Crystal structures of only two fungal chitinases are available [35,36]. The structure model revealed that the fungal

chitinase was an eight-stranded β/α-barrel. The chitinase structure consisted of eight parallel β-strands that form the barrel core surrounded by eight α-helices connected to the barrel, suggesting that the barrel structure of chitinases formed a groove on the enzyme's surface. This groove is considered as the active center which binds sugar units of chitin, possibly (GlcNAc)6 moieties, which are subsequently cleaved [37].

The predicted structure of ChC [**Fig. 7(B)**] hardly suggested significant changes in the tertiary structure of Chit42 [**Fig. 7(A)**] after ChBD addition. But this prediction did not seem to be consistent with the results of the spectroscopic studies. A lower intensity in the fluorescence spectrum of ChC [**Fig. 8(A)**] suggested that tryptophan residues had been quenched to some extent in ChC. Differences in the tertiary structures of Chit42 and ChC became more evident in the corresponding near-CD spectra shown in **Fig. 8(B)**. The outstanding data changed over the range of 260–290 nm indicated structural changes, which made aromatic residues more exposed in ChC. The changes at 260 nm were even more interesting as the added ChBD carried no phenylalanine residue. Far-CD spectra of Chit42 and ChC revealed the depth of the structural changes. The spectra illustrated in **Fig. 8(C)** revealed a remarkable reduction of α-helix content in the secondary structure of ChC (39.2%), when compared with that of Chit42 (81.7%).

Spectroscopic results were not in agreement with what was predicted. Structural prediction result suggested that the added ChBD stood apart from the body of Chit42, while spectroscopic evidence indicated a strong interaction between the added ChBD and Chit42 structure. Assumingly, this interaction brought about a kind of structural change which affected mainly the α-helices moieties, but not the core of the structure where the catalytic hydrolysis is assumed to occur [34,35]. This could explain the similar catalytic efficiencies of both Chit42 and ChC when colloidal chitin was used as substrate.

Similar pH and temperature optima [**Fig. 10(A,B)**] for both Chit42 and ChC might be considered as additional evidence for the assumption that the added ChBD did not affect the core structure of Chit42 where the active site resided.

From an empirical point of view, the binding of chitinase molecules to the surface of insoluble chitin could be regarded as another example of adsorption phenomena. Despite the fact that the adsorption of protein molecules onto the solid surfaces is too complex to be treated by the well-known isotherm adsorption equations usually used for interpretation of small molecules adsorption [38], it could still be informative to examine the isothermal binding data of proteins in the known equilibrium adsorption models. For instance, the binding data of neither Chit42 nor ChC fit the Dubinin–Radushkevich model. When the same binding data of Chit42 were analyzed in Langmuir model, a correlation coefficient of 0.95 was obtained. Similar data have been obtained for the *Candida albicans* chitinase in previous literature [39]. However, in the present study, the binding data of ChC showed obvious deviation from linearity ($r^2 = 0.48$). Interestingly, this difference did not decrease when the data were analyzed by Freundlich equation (1).

$$\ln q_e = (1/n)C_e + \ln K_F \quad (1)$$

C_e shows the concentration (mg/l or M) of solute remaining in solution at equilibrium and q_e is the amount (mol or mg) of solute adsorbed per gram of the adsorbent at equilibrium.

Analysis of binding data of Chit42 by the Freundlich equation yielded a straight line indicating a good fit of isotherm model to experimental data [**Fig. 9(A)**], but similar analysis for ChC binding data failed to produce a straight line ($R^2 = 0.51$). In contrast to Langmuir model, which is based on the assumption of a homogeneous surface containing independent sites for monolayer binding, Freundlich model has the ability to adopt the heterogeneous surface adsorption data [40]. Since both Chit42 and chimeric chitinase were proteins of almost similar sizes, the obvious difference in the linearity might indicate a remarkable difference between the conformational changes of Chit42 and ChC upon binding to the insoluble chitin surface. It was assumed that the joining of ChDB to Chit42 made it a softer protein so that it underwent larger conformational changes. The entropy gain of these structural changes improves the unfavorable condition of binding of chitinase to the surface of insoluble chitin [41,42].

The binding data were also analyzed by the Hill equation (2), which is known for its applicability in the interpretation of data of cooperative binding [43].

$$\mathrm{Ln}\phi = n\ln[S] - \ln K \quad (2)$$

Fractional saturation (ϕ) was defined as the amount of bound protein to each mg of chitin, S shows the concentration of the employed protein, and K is the binding constant.

As expected, the binding data of Chit42 showed a better fit to the Hill equation [**Fig. 9(B)**], when compared with the binding data of ChC [**Fig. 9(C)**]. The lower correlation constant of the Hill plot of ChC was due to the change in the slope at the middle of plot. Such an observation is normally considered as a sign of change in the mode of cooperativity [29]. These results help to understand the deviations observed in the Dixon plots. Under these circumstances, the slope of the fitted line [**Fig. 9(C)**], did not reflect the true nature of cooperativity during binding. To circumvent this problem, it has been suggested to obtain the slope of different parts of the plot separately illustrated in **Fig. 9(D)**. Slope analysis in **Fig. 9(D)** suggested that binding followed a positive cooperativity at concentrations <0.5 μM ChC, then obeyed a negative mode in a range of 0.5–2 μM, and finally returned to positive cooperativity with a steeper slope at

concentrations above 2 μM. In contrast, Chit42 showed a negative cooperativity over the entire range of concentrations examined [**Fig. 9(B)**]. The effect of positive cooperativity was clearly seen in the magnitude of the binding constants extracted from the equations shown in **Fig. 9(B,C)**. These data suggested that the chimeric binding constant was ~700 times larger than that for Chit42.

In conclusion, addition of the ChBD of *S. marcescens* chitinase B to Chit42 was assumingly accompanied by some structural changes. As a result of these structural changes, the binding ability of ChC to insoluble chitin was remarkably enhanced. Its catalytic efficiency was improved and its thermal and chemical stability were increased. Analysis of the kinetic data collected in the presence or absence of an inhibitor revealed deviation from the Michaelis–Menten model. The observed non-linearity was assumed to be due to the complex nature of the binding step. Hill analysis of the binding results suggested that the special tertiary structure of ChC boosted its binding to insoluble chitin through a positive cooperativity mechanism. Findings of this research shed a light on the role of a ChBD in bi-functional chitinases and pave the way for designing chitinases with higher efficiency.

Acknowledgements

Collaboration of Dr D. Morshedi and Mr Ali Akbari in completing some of the molecular experiments is acknowledged and sincerely appreciated.

Funding

This work was supported by a grant form the National Institute of Genetic Engineering and Biotechnology (NIGEB).

References

1 Adams DJ. Fungal cell wall chitinases and glucanases. Microbiology 2004, 150: 2029–2035.
2 Zhang Z, Yuen GY and Sarath G. Chitinases from the plant disease biocontrol agent, *Stenotrophomonas maltophilia* C3. Phytopathology 2001, 91: 204–211.
3 Punja Z. Genetic engineering of plants to enhance resistance to fungal pathogens—a review of progress and future prospects. Can J Plant Pathol 2001, 23: 216–235.
4 Hartl L, Zach S and Seidl-Seiboth V. Fungal chitinases: diversity, mechanistic properties and biotechnological potential. Appl Microbiol Biotechnol 2012, 93: 533–543.
5 Fukamizo T. Chitinolytic enzymes: catalysis, substrate binding, and their application. Curr Protein Pept Sci 2000, 1: 105–124.
6 Punja Z. Recent developments toward achieving fungal disease resistance in transgenic plants. Can J Plant Pathol 2006, 28: 298–308.
7 Dana M, Pintor-Toro J and Cubero B. Transgenic tobacco plants overexpressing chitinases of fungal origin show enhanced resistance to biotic and abiotic stress agents. Plant Physiol 2006, 142: 722–730.
8 Kumar V, Parkhi V, Kenerley CM and Rathore KS. Defense-related gene expression and enzyme activities in transgenic cotton plants expressing an endochitinase gene from *Trichoderma virens* in response to interaction with *Rhizoctonia solani*. Planta 2009, 230: 277–291.
9 Svitil AL and Kirchman DL. A chitin-binding domain in a marine bacterial chitinase and other microbial chitinases: implications for the ecology and evolution of 1,4-beta-glycanases. Microbiology 1998, 144: 1299–1308.
10 Raikhel NV, Lee HI and Broekaert WF. Structure and function of chitin-binding proteins. Annu Rev Plant Physiol 1993, 44: 591–615.
11 Zeltins A and Schrempf H. Specific interaction of the *Streptomyces* chitin-binding protein CHB1 with alpha-chitin-the role of individual tryptophan residues. Eur J Biochem 1997, 246: 557–564.
12 Harighi MJ, Motallebi M and Zamani MR. Antifungal activity of heterologous expressed chitinase 42 (Chit42) from *Trichoderma atroviride* PTCC5220. Iran J Biotechnol 2006, 4: 95–103.
13 Fan Y, Fang W, Guo S, Pei X, Zhang Y, Xiao Y and Li D, *et al*. Increased insect virulence in *Beauveria bassiana* strains overexpressing an engineered chitinase. Appl Environ Microbiol 2007, 73: 295–302.
14 Limon MC, Chacon MR, Mejias R, Delgado-Jarana J, Rincon AM, Codon AC and Benitez T. Increased antifungal and chitinase specific activities of *Trichoderma harzianum* CECT 2413 by addition of a cellulose binding domain. Appl Microbiol Biotechnol 2004, 64: 675–685.
15 Limon MC, Margolles-Clark E, Benitez T and Penttila M. Addition of substrate-binding domains increases substrate-binding capacity and specific activity of a chitinase from *Trichoderma harzianum*. FEMS Microbiol Lett 2001, 198: 57–63.
16 Sambrook J, Fritsch E and Maniatis T. Molecular Cloning: A Laboratory Manual. New York: Cold Spring Harbor Laboratory Press, 1989.
17 Van Aalten DMF, Synstad B, Brurberg MB, Hough E, Riise BW, Eijsink VGH and Wierenga RK. Structure of a two-domain chitotriosidase from *Serratia marcescens* at 1.9-Å resolution. PNAS 2000, 97: 5842–5847.
18 Horton RM. PCR-mediated recombination and mutagenesis SOEing together tailor-made genes. J Mol Biotechnol 1995, 3: 93–99.
19 Hoffmann A and Roeder RG. Purification of his-tagged proteins in non-denaturing conditions suggests a convenient method for protein interaction studies. Nucleic Acids Res 1991, 19: 6337–6338.
20 Farhadi S, Haghbeen K, Marefatjo MJ, Hoor MG, Zahiri HS and Rahimi K. Anionic peroxidase production by *Arnebia euchroma* callus. Biotechnol Appl Biochem 2011, 58: 456–463.
21 Bruce A, Srinivasan U, Staines HJ and Highley TL. Chitinase and laminarinase production in liquid culture by *Trichoderma spp*. and their role in biocontrol of wood decay fungi. Int Biodeter Biodegr 1995, 35: 337–353.
22 Berger LR and Reynolds DM. Colloidal chitin preparation. Methods Enzymol 1988, 6: 140–142.
23 Gheibi N, Saboury AA, Haghbeen K and Moosavi-Movahedi AA. The effect of some osmolytes on the activity and stability of mushroom tyrosinase. J Biosci Bioeng 2006, 31: 355–362.
24 Krokeide IM, Synstad B, Gaseidnes S, Horn SJ, Eijsink VGH and Morten S. Natural substrate assay for chitinases using high-performance liquid chromatography: a comparison with existing assays. Anal Biochem 2007, 363: 128–134.
25 Oguchi M and Oguchi MS. Tetraborate concentration on Morgan-Elson reaction and an improved method for hexosamine determination. Anal Biochem 1979, 98: 433–437.
26 Takahashi T, Ikegami-Kawai M, Okuda R and Suzuki K. A fluorimetric Morgan-Elson assay method for haylruronidase activity. Anal Biochem 2003, 92: 257–263.

27 Shubakov AA and Kucheryavykh PS. Chitinolytic activity of filamentous fungi. Appl Biochem Microbiol 2004, 40: 445–447.
28 Kim KH and Ji HS. Effect of chitin sources on production of chitinase and chitosanase by *Streptomyces griseus* HUT 6037. Biotechnol Bioproc Eng 2001, 6: 18–24.
29 Cornish-Bowden A. Fundamentals of Enzyme Kinetics. 2nd edn. London: Portland Press, 1995.
30 Haghbeen K, Babaei Khalili M, Saeid Nematpour F, Gheibi N, Fazli M, Alijanianzadeh M and Zolghadri Jahromi S, *et al*. Surveying allosteric cooperativity and cooperative inhibition in mushroom tyrosinase. J Food Biochem 2010, 34: 308–327.
31 Bade ML and Stinson A. A homotropic allosteric enzyme. Biochem Biophys Res Commun 1979, 87: 349–353.
32 Yang J, Gan Z, Lou Z, Tao N, Mi Q, Liang L and Sun Y, *et al*. Crystal structure and mutagenesis analysis of chitinase CrChi1 from the nematophagous fungus *Clonostachys rosea* in complex with the inhibitor caffeine. Microbiology 2010, 156: 3566–3574.
33 Rao FV, Andersen OA, Vora KA, DeMartino JA and Van Aalten DMF. Methylxanthine drugs are chitinase inhibitors: investigation of inhibition and binding modes. Chem Biol 2005, 12: 973–980.
34 Horn SJ, Sikorski P, Cederkvist JB, Vaaje-Kolstad G, Sorlie M, Synstad B and Vriend G, *et al*. Costs and benefits of processivity in enzymatic degradation of recalcitrant polysaccharides. PANS 2006, 103: 18089–18094.
35 Hollis T, Monzingo AF, Bortone K, Ernst S, Cox R and Robertus JD. The X-ray structure of a chitinase from the pathogenic fungus *Coccidioides immitis*. Protein Sci 2000, 9: 544–551.
36 Drouillard S, Armand S, Davies GJ, Vorgias CE and Henrissat B. *Serratia marcescens* chitobiase is a retaining glycosidase utilizing substrate acetamido group participation. Biochem J 1997, 328: 945–949.
37 Bordoli L, Kiefer F, Arnold K, Benkert P, Battey J and Schwede T. Protein structure homology modeling using SWISS-MODEL workspace. Nature protocols 2009, 4: 1–13.
38 Kim JH and Yoon JY. Protein adsorption on polymer particles. In: Hubbard A ed. Encyclopedia of Surface and Colloid Science. New York: Marcel Dekker, 2002.
39 Barrett-Bee K and Hamilton M. The detection and analysis of chitinase activity from the yeast form of *Candida albicans*. J General Microbiol 1984, 130: 1857–1861.
40 Haghbeen K and Legge RL. Adsorption of phenolic compounds on some hybrid xerogels. Chem Eng J 2009, 150: 1–7.
41 Roach P, Farrar D and Perry CC. Interpretation of protein adsorption: surface-induced conformational changes. J Am Chem Soc 2005, 127: 8168–8173.
42 Van der Veen M, Stuart MC and Norde W. Spreading of proteins and its effect on adsorption and desorption kinetics. Colloids Surf B 2007, 54: 136–142.
43 Weiss JN. The Hill equation revisited: uses and misuses. FASEB J 1997, 11: 835–841.